Magnetic Islands in NCSX and their Suppression by Plasma Flow

A. Reiman, S. Hudson, L. Ku, D. Monticello, D. Mikkelsen,
H. Mynick, P. Rutherford, M. Zarnstorff
PPPL

- NCSX configuration chosen in part because of its good flux surfaces.
- PIES calulations do not take into account neoclassical effects or shielding by plasma flow.
- Evaluation of island effects must also include finite $\chi_\perp / \chi_{//}$,
- Resonant magnetic field perturbations can be shielded out at rational surfaces by plasma flow. Effect believed to play major role in reducing vulnerability of tokamaks to resonant field errors.
- NCSX stellarator predicted to have strong plasma flow.
  We estimate significance of shielding effect for NCSX.

Configuration 383 has greatly improved surfaces.

β = 4.2%, full current. fixed boundary calculation.

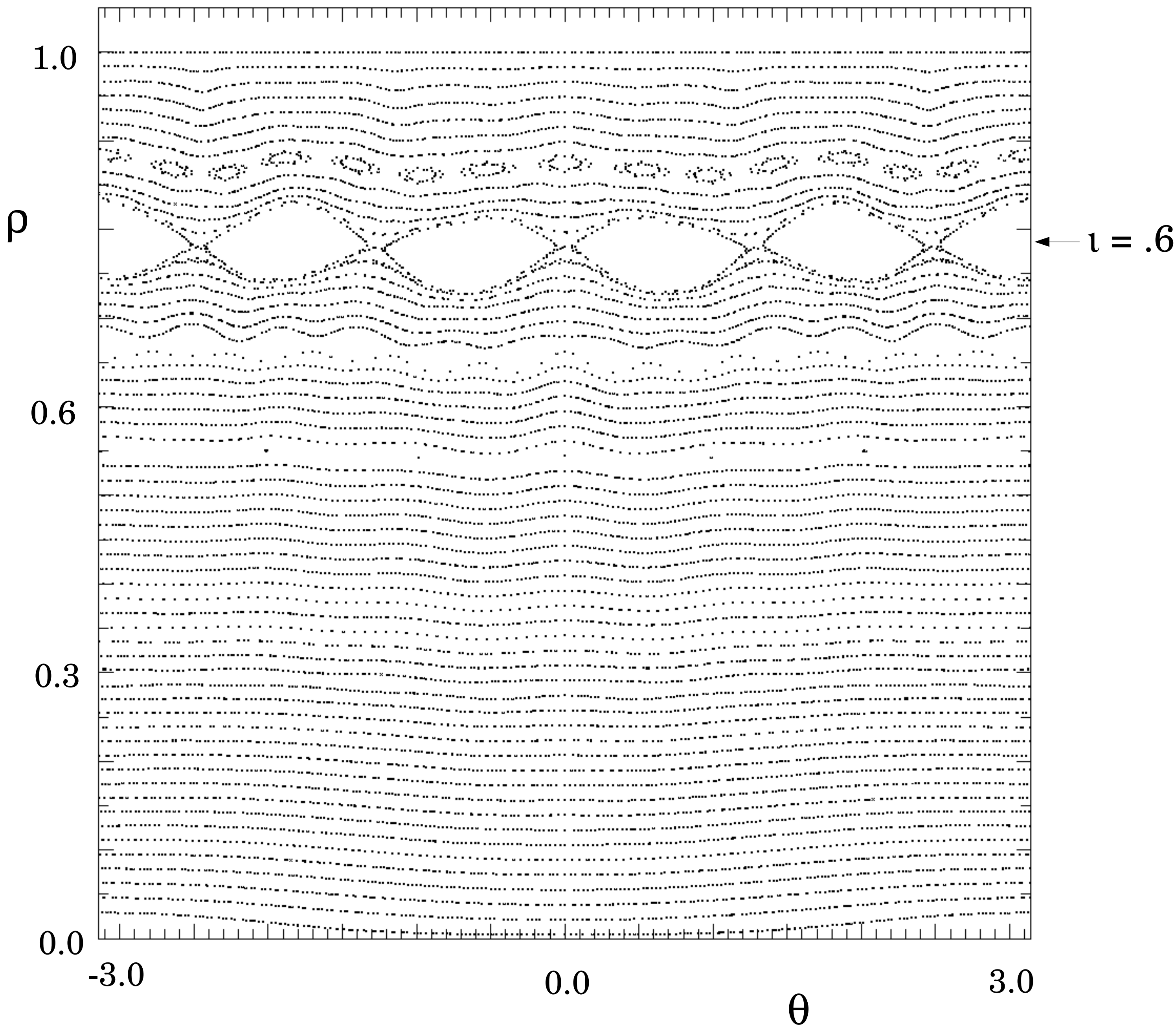

- total island width ≈ 15% (10% regarded as acceptable.)
- Calculation does not include stabilizing neoclassical effect.
- No broad stochastic region.
  Dominated by single island chain. Can improve by modifying resonant Fourier component of boundary.

Coil Design Has Been Modified to Produce Good Surfaces

- "Dynamic healing" algorithm modifies coils in each PIES iteration to suppress targeted islands.
- Preserves engineering and physics constraints on coil curvature, minimum distance between coils, kink stability. (Stable up to n=45. Ballooning restabilized in startup scenario.)

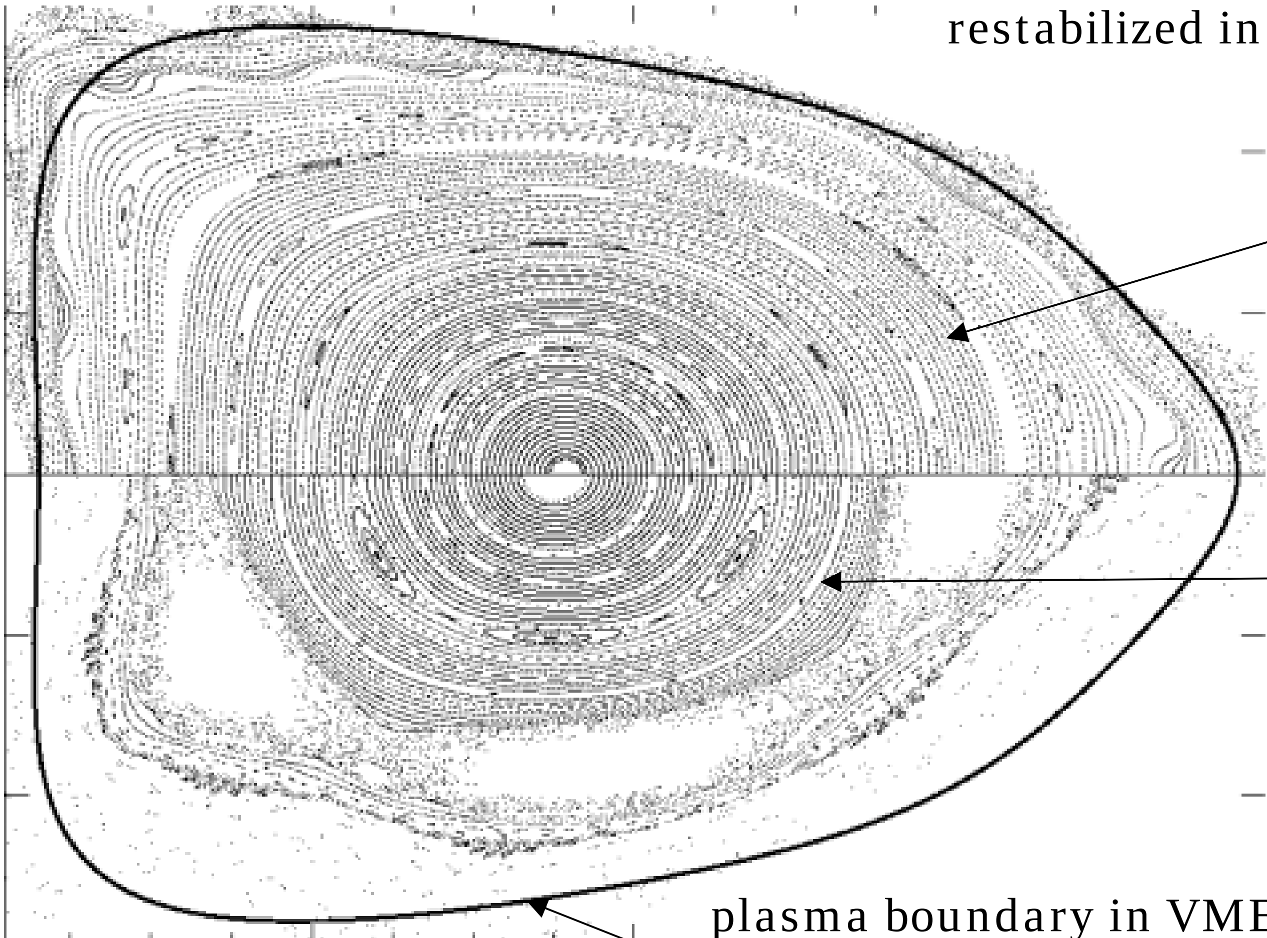

Neoclassical Effect Reduces Island Widths in NCSX

- Gives neoclassical tearing mode in tokamaks ($\iota' < 0$).
- For $\iota' > 0$, effect predicted to reduce NCSX island widths.

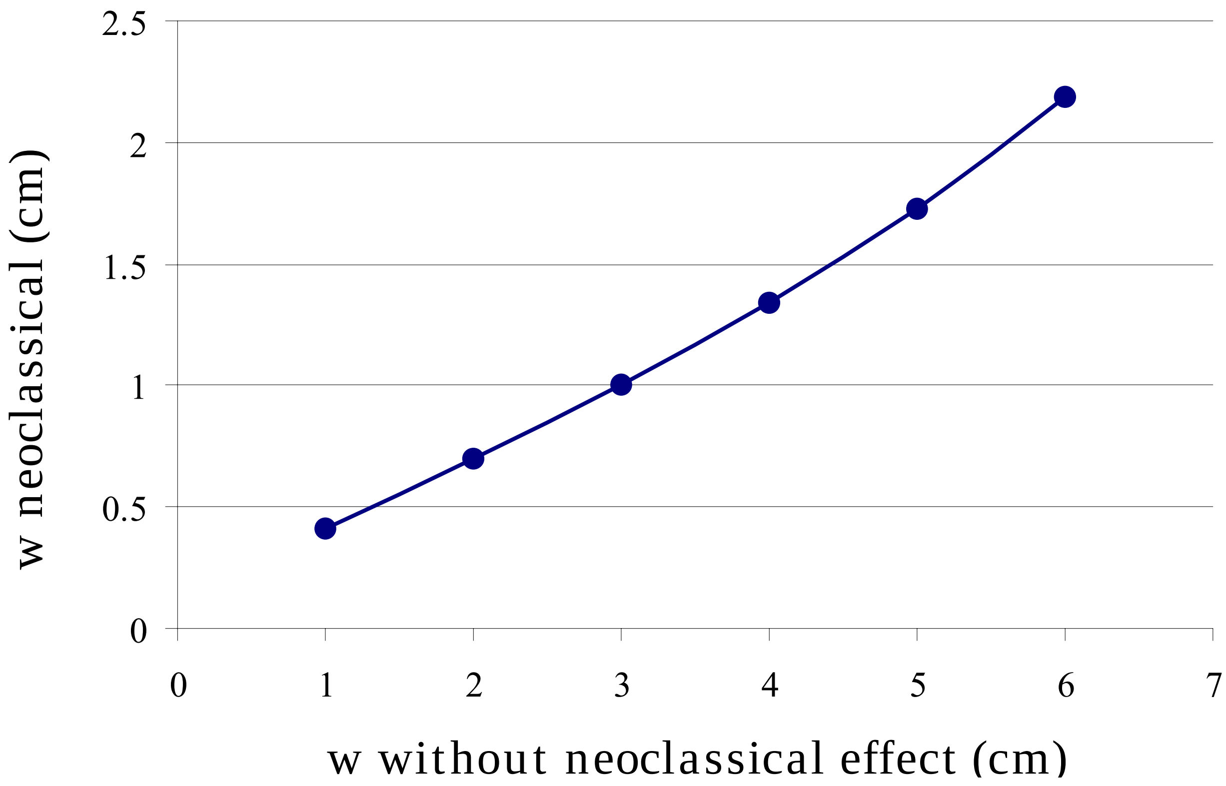

Effect estimated for island at $\iota = 0.6$ surface. Analytic calculation in cylinder. Estimate $\Delta' = -2\ m / r$. Take $\beta = 4.2\%$, $B = 1.2$ T, $\langle n_e \rangle = 5.8 \times 10^{19}\ m^{-3}$.

- Evaluation of effective island widths takes into account finite $\chi_\perp / \chi_{//}$ effect, as well as neoclassical effect.

Small Islands Have Little Effect on Transport

- Large islands short-circuit confinement by allowing heat to flow along separatrix.

- For narrow islands, path length along field line long, and parallel conductivity prevents short-circuiting of confinement.
- Critical island width at which transport due to island is comparable to cross-field transport: $w_0 \approx 5\,(\chi_\perp / \chi_{//})^{0.25}\,(RL_\iota / m\iota)^{0.5}$, where L_ι is shear scale length.
- Estimate $w_0/a \approx 3.5\%$ for m=5 island in NCSX. (At $\beta = 4.2\%$, B = 1.2 T, $\langle n_e \rangle = 5.8 \times 10^{19}\ m^{-3}$)
- In calculating flux surface loss, use effective island width $w/(1+(w_0/w)^4)$. (Effective diffusivity across island $\chi \approx \chi_\perp(1+(w/w_0)^4)$).

Summary of Effective Flux Surface Loss for PIES Calculations

(Details in Physics Design Document)

	case	β (%)	Loss of surfaces at edge (%)	Sum of effective island widths (%)	Total effective flux surface loss (%)
Reference case	S3	4.1	0	<1	<1
Vacuum cases	vac1	0	3.1	<1	3.1
	vac2	0	10.4	<1	10.4
	vac3	0	5.2	<1	5.2
	vac4	0	<1	<1	<1
	vac5	0	2	<1	2.0
Startup snapshots	t=50	1.2	6.2	3.8	10.0
	t=100	3.4	0	10.1	10.1
	t=116	3.7	0	5.5	5.5
	t=139	3.9	11.4	1.2	12.6
	t=303	4.6	0	2.5	2.5

- Expect further improvements using trim coils.

Effect of Flow on Penetration of Resonant Field, δB

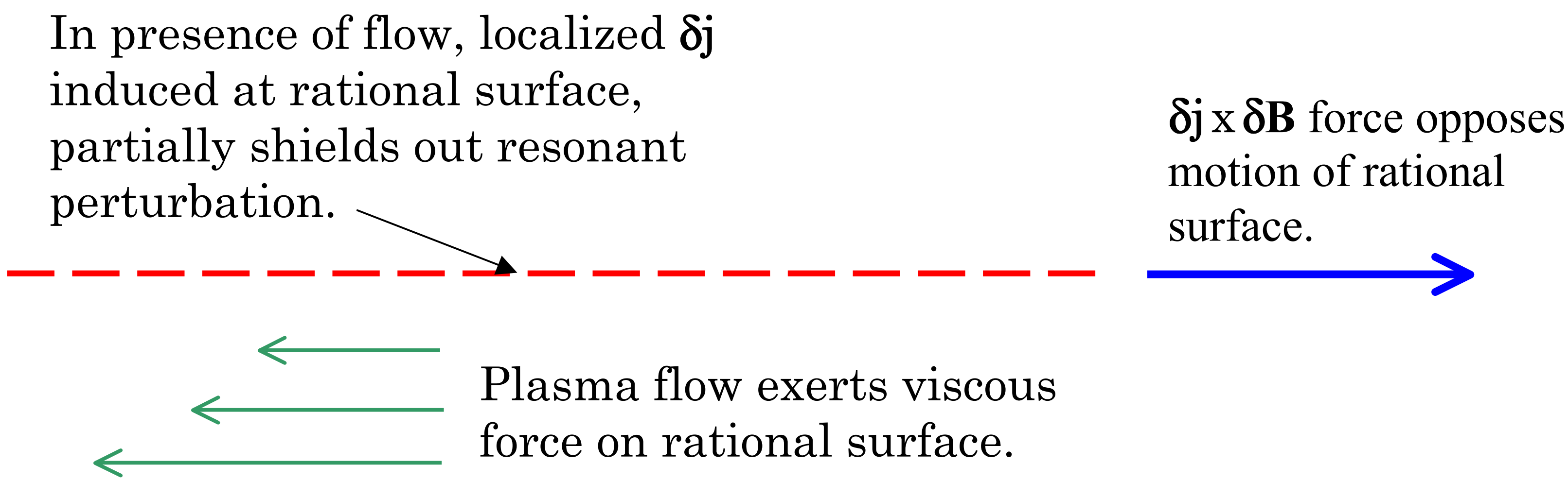

- When resonant perturbation sufficiently large, **δj** x **δB** torque becomes large enough to locally suppress plasma flow, allowing resonant perturbation to fully penetrate rational surface.

- Threshold for penetration of resonant field perturbations determined by relative magnitudes of electromagnetic torque and of torques associated with the plasma flow.

Transport Calculated Using Mikkelsen-Zarnstorff 1D Transport Code

Power fluxes divided into three parts, $q_{tot} = q_{ripple}^{neo} + q_{axisym.}^{neo} + q_{anom.}$, neoclassical ripple, axisymmetric transport, and 'anomalous' transport.

Analytic neoclassical ripple model based on single helicity magnetic configuration. Effective ripple amplitude, ε_{eff}, calculated by NEO code using the full 3-D magnetic configuration (Nemov, Kernbichler).

Chang-Hinton model used for neoclassical axisymmetric transport, and has been re-normalized to THRIFT/NCLASS (Strand/Houlberg).

Anomalous transport modeled with either radially uniform diffusivity, or the version of the Lackner-Gottardi model that has been applied to W7-AS.

Validated by benchmarking against GTC Monte Carlo code.

Ripple driven flux peaks for E_r=0, near edge

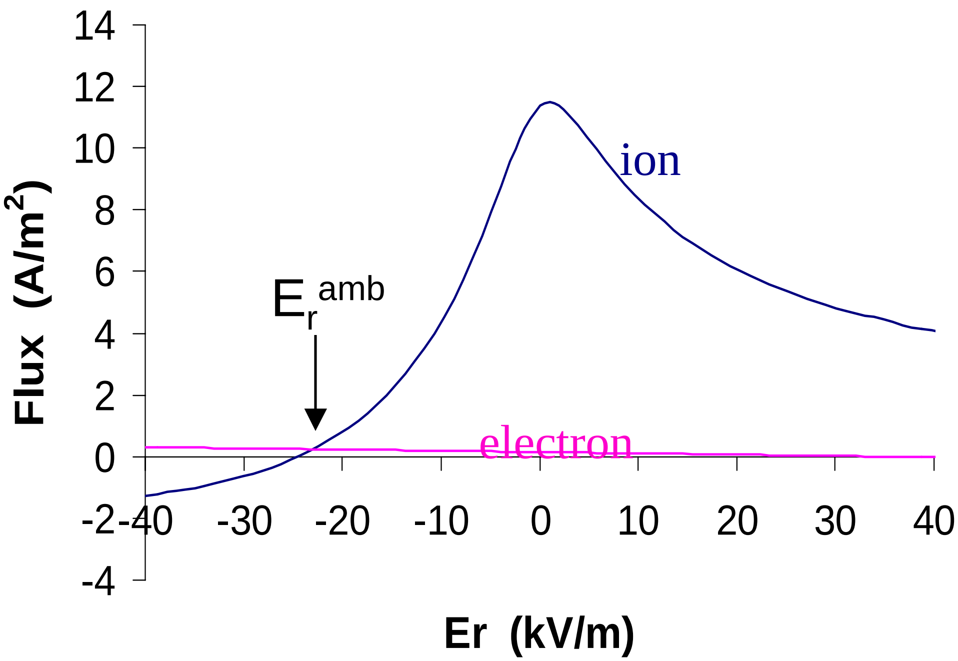

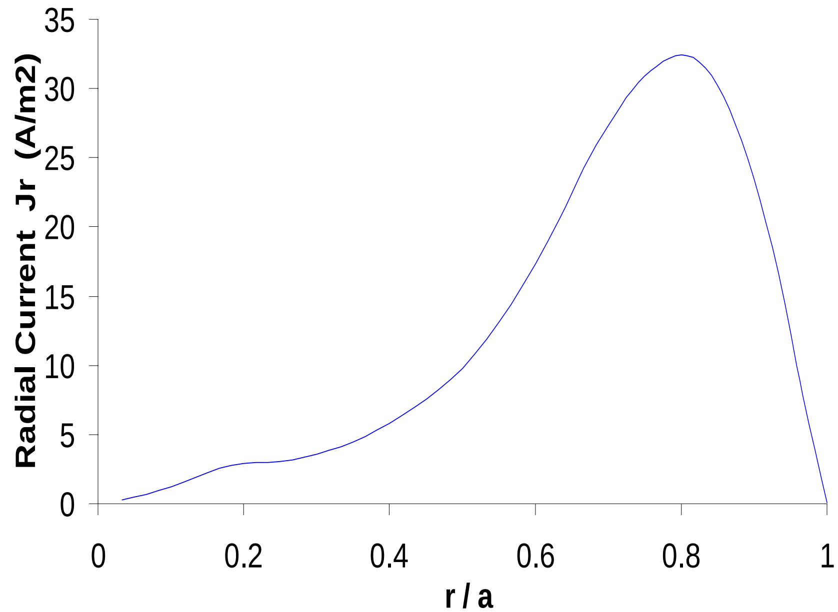

- Ripple-neoclassical model predicts radial currents for $E_r \neq E_r^{amb}$, due to deviations from quasi-axisymmetry; benchmarked to Monte-Carlo (GTC)
- For $E_r \neq E_r^{amb}$, $J_r \propto (\Gamma_i - \Gamma_e)$ acts to restore E_r^{amb} and damp rotation, $J_r \times B_P$ back to ambipolar value.
- At each radius, peak , $J_r \propto (\Gamma_i - \Gamma_e) \sim \Gamma_i$ occurs for $E_r = 0$

Ambipolar $E_r \Rightarrow$ large v_ϕ

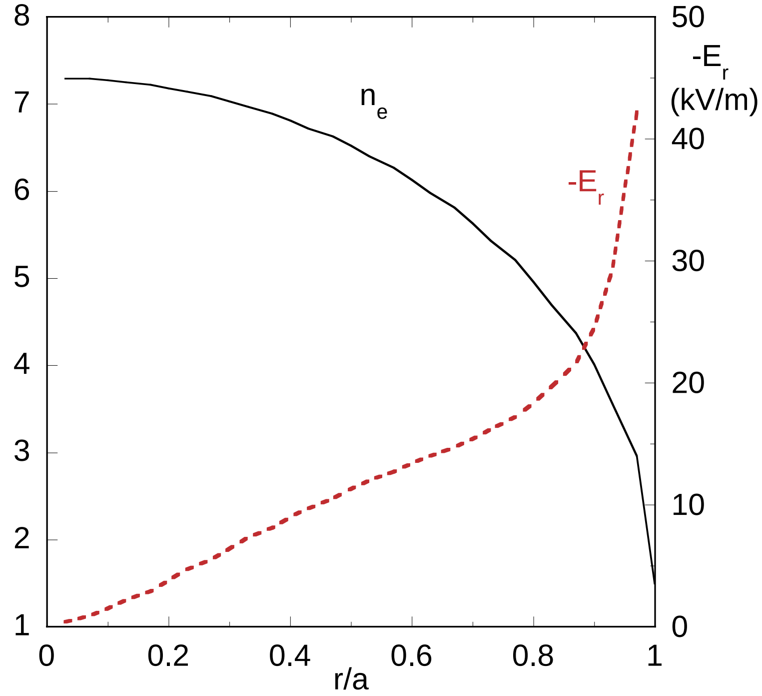

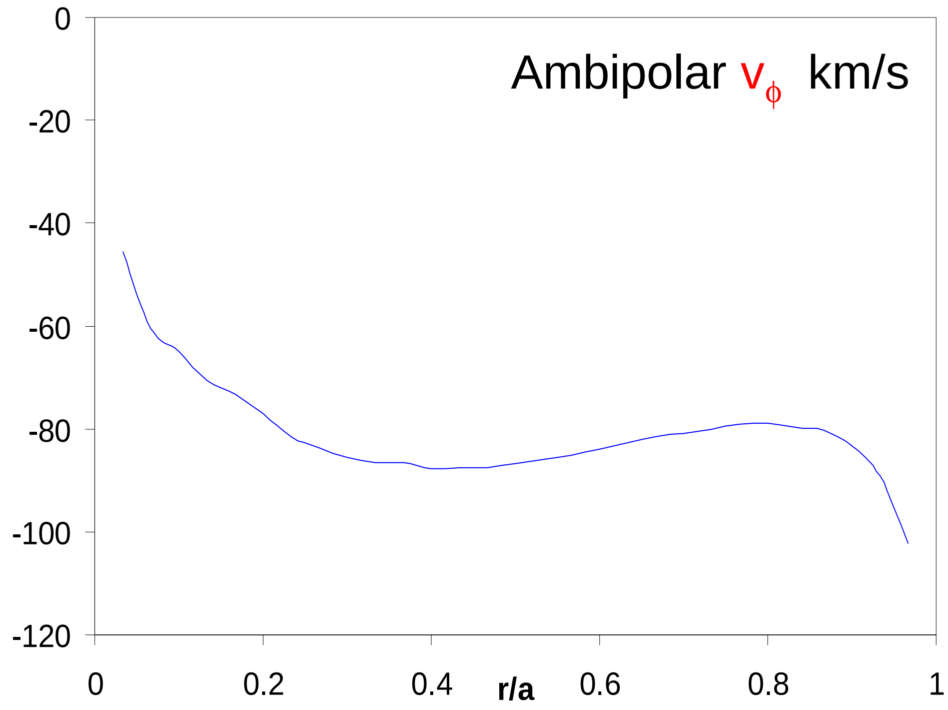

- No applied torque.
- Ambipolar E_r peaks at edge due to edge ripple.

  Calculation does not include flow damping due to neutrals.
- Assumes poloidal damping much faster than toroidal, $\Rightarrow$tokamak-like solution $v_\phi \sim E_r/B_P$.
- v_ϕ preliminary: want to verify with Monte-Carlo codes

Torque Produced by the Plasma Flow (continued)

- Focus on $\iota = .6$ rational surface. (Low order rational near edge.)
  Ambipolar $E_r \approx 20$ kV/m, v ≈ 85 km /sec.
- At rational surface $j_r \approx 3$ A/m^2, exerts torque density ≈ 15 Nt.
  Effect of this **j x B** torque much smaller than that of viscous force.
- Viscous torque $T_\phi \approx 2\pi^2 r R^2 \rho\mu v_0 / l$ where v_0 is velocity corresponding to ambipolar potential and l is scale length of velocity gradient.
- Velocity gradient determined by steady-state solution of momentum diffusion equation, with torque exerted by radial current as source term.
- Approximate v dependence of j_r as linear, $j_r \approx \alpha(v - v_0)$.
  $\rho\mu d^2(v - v_0)/dr^2 = \alpha B_p (v - v_0)$, with $v = v_0/2$ at rational surface.
- Estimating $\tau_E \approx 25$ ms gives $l \approx 6$ cm.

Electromagnetic Torque

- Nonresonant Fourier components of perturbation only produce small ripples in flux surfaces. Do not affect localized current and associated torque.

Express unperturbed magnetic field in magnetic coordinates:

$$\mathbf{B}_0 = \nabla\Psi_0 \times \nabla\theta + \iota\nabla\Psi_0 \times \nabla\varphi$$

$$\mathbf{B}_0\cdot\nabla\varphi \left(\partial\, \delta\Psi / \partial\varphi + \iota\, \partial\, \delta\Psi / \partial\theta \right) = -\boldsymbol{\delta}\mathbf{B}\cdot\nabla\Psi_0$$

$$(n - \iota\, m)\, \delta\Psi_{nm} = -(\boldsymbol{\delta}\mathbf{B}\cdot\nabla\Psi_0 / \mathbf{B}_0\cdot\nabla\varphi)_{nm}$$

- Resonant Fourier component ($n = \iota m$) breaks flux surface and produces magnetic island. Induced current at rational surface partially shields out resonant component of $\delta B\cdot\nabla\Psi_0 / B_0\cdot\nabla\varphi$.
- Induced current interacts with resonant magnetic field to produce electromagnetic torque.

Electromagnetic Torque (continued)

- For given plasma flow velocity, penetration of resonant field determined primarily by 1D layer physics (R. Fitzpatrick, Nucl. Fusion **33**, (1993) and Phys. Plasmas **5**, (1998)). Approximately the same in stellarators as in tokamaks.

Penetration of Resonant Perturbations in NCSX

- Penetration determined by ratio of electromagnetic and viscous forces.
- First consider penetration threshold relative to that of neutral beam heated tokamak with same parameters (including rotation frequency):
  - Difference in velocity gradient scale length gives penetration threshold 1.6 times that of tokamak
- Next, consider scaling of penetration threshold relative to that observed in DIII-D experiment.
  - Comparison shot chosen so that most key parameters approximately equal. Those that are not are: aspect ratios (4.3 vs 2.1), mode no. of perturbation (5/3 vs 2/1), $s = r\, q'/q$ (.4 vs 1.0).
  - Theory predicts ≈ 40% effects of individual parameter differences, but in canceling directions, so that overall effect is small.
- Penetration threshold predicted to be approximately 1.6 times that in DIII-D, $B_{rnmc}/B \approx 6 \times 10^{-4}$.

We compare NCSX with reference DIII-D shot where penetration threshold for resonant magnetic perturbation studied experimentally.

Reference Parameters for NCSX and DIII-D Comparison Shot

	NCSX	DIII-D reference shot
R	1.42 m	1.67 m
B	1.2 T	1.2 T
R/⟨a⟩	4.3	2.1
average ($n = 0$) ellipticity	1.8	1.8
density ⟨n⟩	6×10^{19} m^{-3}	5×10^{19} m^{-3}
⟨β⟩	4%	3.7%
rotation frequency	9 kHz	12 kHz

Discussion

- NCSX configuration selected in part for good fixed boundary flux surfaces. (Evaluations performed with PIES code.)
- Coil design has been modified to give good free-boundary flux surfaces while preserving desired physics and engineering properties. (see Stuart Hudson talk.)
- Evaluations taking into account neoclassical and finite $\chi_{\perp} / \chi_{//}$ effects indicate acceptable flux surfaces for a range of free-boundary equilibria.
- Strong predicted ambipolar flow in NCSX potentially helpful for further reducing vulnerability to resonant magnetic fields, and for increasing range of operation of device with acceptable flux surfaces.
- To take advantage of this effect, will need to develop appropriate startup scenarios.

- Effect not strong enough to suppress resonant perturbations arising in coil design.
  - Unhealed NCSX coils had $B_{rnm} / B \approx 1.3\text{x}10^{-3}$.

    (Calculated by initializing PIES code with VMEC solution.)
- NCSX trim coils & flexibility to vary ripple amplitude and ι profile will allow experimental study of shielding due to ambipolar flow.